Synthesis and Reactions of *meso*- and *dl*-D_3-Trishomocubylidene-D_3-trishomocubane

Alan P. Marchand,*,† G. Madhusudhan Reddy,† Mahendra N. Deshpande,† William H. Watson,*,‡ Ante Nagl,‡ Oh Seuk Lee,§ and Eiji Ōsawa*,§

Contribution from the Department of Chemistry, University of North Texas, Denton, Texas 76203-5068, the Department of Chemistry, Texas Christian University, Fort Worth, Texas 76129, and the Department of Chemistry, Faculty of Science, Hokkaido University, Sapporo 060, Japan. *Received April 26, 1989. Revised Manuscript Received December 2, 1989*

Abstract: Titanium-promoted reductive coupling of D_3-trishomocubanone affords *meso*- and *dl*-D_3-trishomocubylidene-D_3-trishomocubane (**2a** and **2b**, 60%) and D_3-trishomocubanol (**3**, 25%). The structures of **2a** and **2b** were elucidated by X-ray crystallographic methods. Reaction of a ca. 1:1 mixture of **2a** and **2b** with a chloroform solution of trifluoroacetic acid at room temperature for 2.5 h afforded the corresponding 1,2-adduct (**4b**, 39%) along with isomerically pure, unreacted **2a** (46%). The corresponding reaction of **2a**, when performed at reflux for 48 h, afforded an extensively rearranged spirocyclic trifluoroacetate adduct, **4a** (30%), along with recovered **2a** (40%). The structure of **4a** was established via X-ray crystallographic analysis of the corresponding alcohol, **5**, that resulted via lithium aluminum hydride reduction of **4a**. Electrophilic bromination of **2b** with Br_2–CCl_4 solution proceeded smoothly at room temperature to produce the corresponding 1,2-adduct, **9** (80%), whose structure was established unambiguously by X-ray crystallography. By way of contrast, the corresponding reaction of **2a**, when performed at room temperature for 24 h, gave a spiroketone, **10a** (70%). On the basis of results of MM2 and AM1 computations, the observed differences between the reactivities of the C=C double bonds in **2a** and **2b** toward electrophiles can be rationalized in terms of a secondary steric effect that is a consequence of the molecular symmetries of **2a** and **2b**. Thus, as the degree of pyramidalization of the sp^2-hybridized carbon atoms increases with reaction progress, the resulting internal congestion in the region behind the C=C double bond becomes unbearably large in **2a** but remains relatively small in **2b**.

Saturated polycyclic "cage" hydrocarbons, by virtue of their highly compact (and, often, highly strained) structures, are of interest as a potential new class of high-energy/high-density fuels.[1a] As part of an ongoing program that is concerned with the synthesis and chemistry of novel polycyclic cage compounds,[1b] we have undertaken a study of the titanium-promoted dimerization[2] of D_3-trishomocubanone[3] (**1**). As expected, this reaction afforded two alkene dimers, i.e., *meso*- and *dl*-D_3-trishomocubylidene-D_3-trishomocubane (**2a** and **2b**, 60%, Scheme I) along with D_3-trishomocubanol[4] (**3**, 25%). The isomeric alkene dimers were separated by careful column chromatography followed by fractional recrystallization from hexane. The melting points of the two compounds differ significantly; the meso isomer (**2a**) displays mp 246 °C, whereas the corresponding *dl* isomer (**2b**) displays mp 186 °C. The structure of each isomer was determined by single crystal X-ray structural analysis (Figure 1). These two isomers also possess significantly different crystal densities (1.302 and 1.269 g cm^{-3}, respectively, calculated from X-ray crystallographic data).

In view of the fact that **2a** and **2b** possess markedly different physical properties, we decided to investigate some aspects of their chemistry. Initially, the electrophilic addition of trifluoroacetic acid (TFA) to the carbon–carbon double bond in **2a** and in **2b** was studied. Reaction of a ca. 1:1 mixture of **2a** and **2b** with a chloroform solution of TFA at room temperature for 2.5 h afforded an adduct, **4b** (39% yield, Scheme II). In addition, pure unreacted **2a** was recovered from this reaction in 46% yield. The ^{13}C NMR spectrum of **4b** revealed the presence of a singlet at δ 100.02, thereby indicating the presence of a quaternary carbon attached to oxygen in this compound. This observation suggests that **4b** was formed via exclusive 1,2-addition of the electrophile to the C=C functionality in **2b**. Although D_3-trishomocubane itself is a chiral molecule, carbon atoms C(4) and C(4′) in **4b** are *not* asymmetric. Therefore, it is not possible to deduce whether **4b** results via syn or anti addition of TFA to the C=C double bond in **2b**.

The corresponding reaction of isomerically pure **2a** with TFA required more drastic conditions. Thus, when a solution of **2a** in TFA–chloroform was refluxed for 48 h, an adduct, **4a** (Scheme

Scheme I

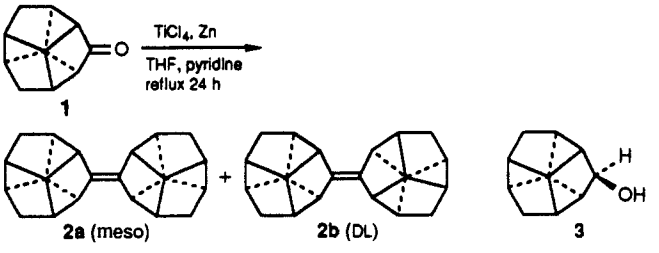

Scheme II

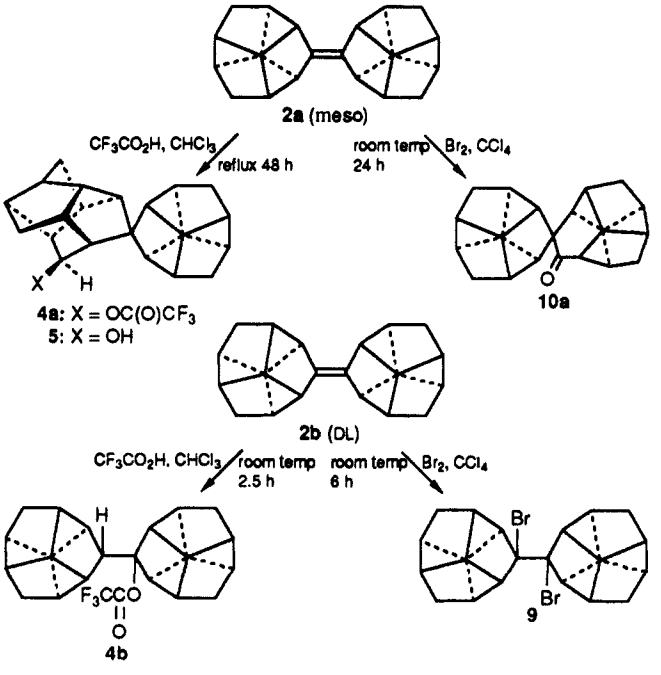

† University of North Texas.
‡ Texas Christian University.
§ Hokkaido University.

0002-7863/90/1512-3521$02.50/0

Scheme III

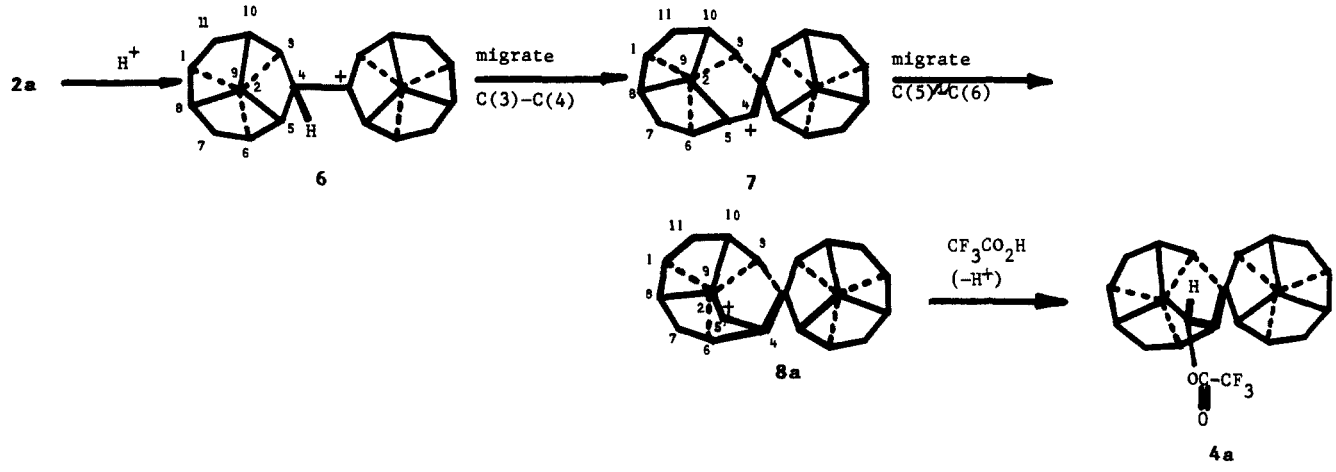

II), was produced in 30% yield along with recovered starting material (40%). The ^{13}C NMR spectrum of **4a** contains a doublet at δ 78.47, consistent with the presence of a $CHOC(O)CF_3$ moiety in this compound. In addition, there is a singlet resonance at δ 60.63, which indicates the presence of a quaternary carbon atom in **4a**. These two observations suggest that **4a** is spirocyclic.

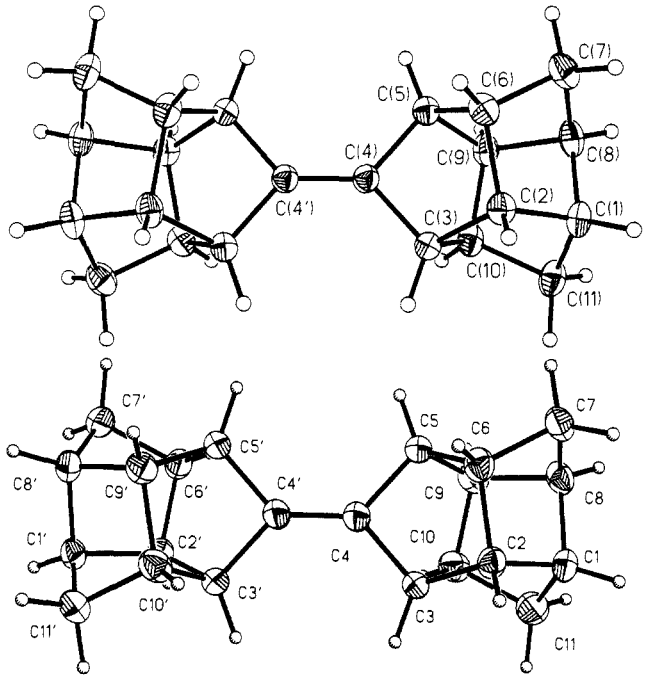

Figure 1. (Top) structure drawing of **2a**; (bottom) structure drawing of **2b**.

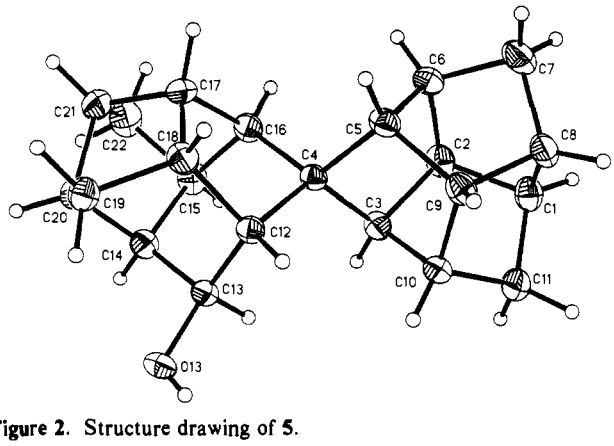

Figure 2. Structure drawing of **5**.

Unequivocal determination of the structure of **4a** was obtained via X-ray crystallographic analysis of the corresponding alcohol, **5**, obtained by lithium aluminum hydride reduction of **4a** (see Figure 2).

A mechanism that accounts for the formation of **4a** in this reaction is shown in Scheme III. Apparently, the initial carbocation, **6**, that results from protonation of the C=C double bond in **2a** suffers *two* successive Wagner–Meerwein rearrangements before finally being trapped by solvent (i.e., **6** → **7** → **8a**). The results of MM2 calculations[5] reveal that, of the four carbocationic intermediates, **8a–d**, that potentially could result via subsequent Wagner–Meerwein rearrangement of **7**, the one that is favored thermodynamically is **8a** (see Figure 3). Indeed, the product, **4a**, of the reaction of **2a** with TFA–$CHCl_3$ results via exclusive capture of carbocation **8a** by TFA.

Electrophilic bromination of **2b** also was studied. When isomerically pure **2b** was reacted with excess bromine–carbon tetrachloride solution at room temperature, a single adduct, **9** (Scheme II), was isolated in 80% yield. The structure of **9** was established by single-crystal X-ray structural analysis (Figure 4). For reasons given above for the example of TFA addition to the C=C double bond in **2b**, once again it is not possible to deduce the stereochemistry of addition of the electrophile (here, bromine) to the C=C double bond in **2b**, even though the structure of the bromine addition product, **9**, is known.

The meso alkene dimer **2a** also reacted with excess bromine–carbon tetrachloride solution at room temperature, although longer reaction time was required for complete reaction as compared with the corresponding reaction of **2b** with Br_2–CCl_4. The product obtained from the reaction of **2a** with Br_2–CCl_4, after chromatographic workup, was not a simple 1,2-addition product, but instead it was found to be rearranged spiroketone **10a** (Scheme II).

The structure of **10a** thereby obtained was established by using the method shown in Scheme IV. Reductive coupling of **1** with sodium in refluxing xylene afforded a 1:1 mixture of pinacols **11a** and **11b** (44%) along with **3** (20%). Acid-promoted pinacol rearrangement of isomerically pure **11a** and **11b** produced spiroketones **10a** and **10b**, respectively. The structure of **10b** was established by single-crystal X-ray structural analysis.[6] The

(1) (a) Burdette, G. W.; Lander, H. T.; McCoy, J. R. *J. Energy* **1979**, *2*, 289. (b) See: Marchand, A. P. In *Advances in Theoretically Interesting Molecules*; Thummel, R. P., Ed.; JAI: Greenwich, CT, 1989; Vol. 1, pp 357–399 and references cited therein.

(2) (a) Lenoir, D. *Synthesis* **1977**, 553. (b) For a review of titanium-promoted dicarbonyl coupling reactions, see: McMurry, J. E. *Acc. Chem. Res.* **1983**, *16*, 405 and references cited therein.

(3) Eaton, P. E.; Hudson, R. A.; Giordano, C. *J. Chem. Soc., Chem. Commun.* **1974**, 978.

(4) Dekker, T. G.; Oliver, D. W. *S. Afr. J. Chem.* **1979**, *32*, 45.

(5) Burkert, U.; Allinger, N. L. *Molecular Mechanics*; ACS Monograph No. 177, American Chemical Society: Washington, DC, 1982.

(6) Marchand, A. P.; Reddy, G. M.; Watson, W. H.; Nagl, A. *Acta Crystallogr., Sect. C: Cryst. Struct. Commun.* **1990**, *46*, 253.

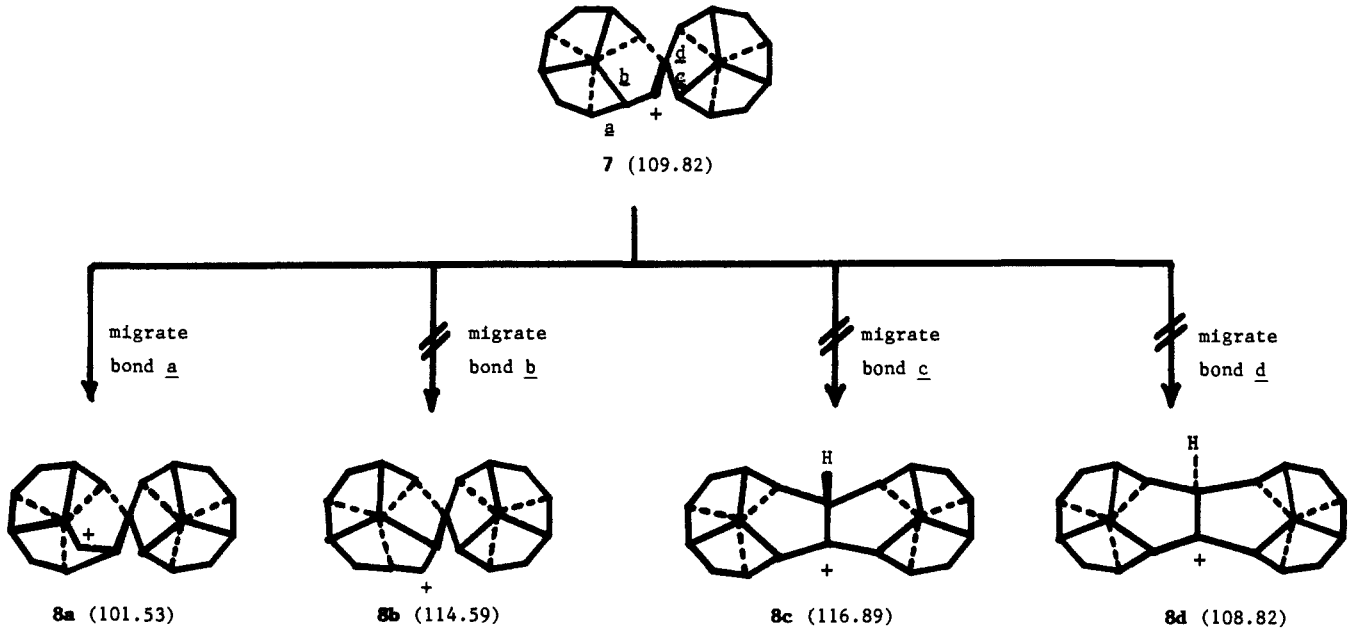

Figure 3. Calculated (MM2) energies of carbocations **8a–d** (kcal/mol).

Scheme IV

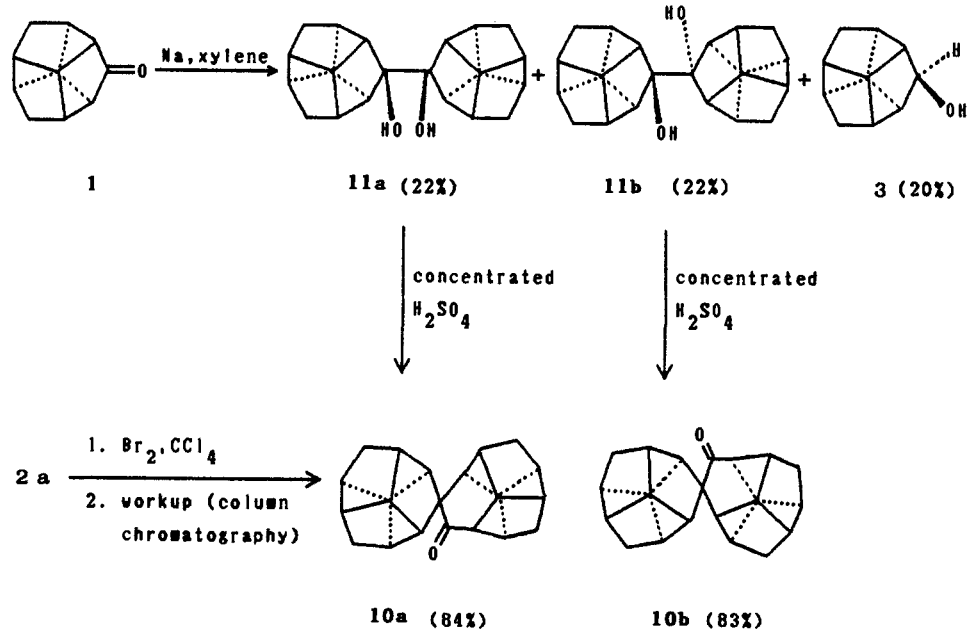

material obtained via reaction of **2a** with Br_2–CCl_4 solution was identical in all respects with **10a** that had been generated via pinacol rearrangement of **11a** (see Scheme IV and Experimental Section).

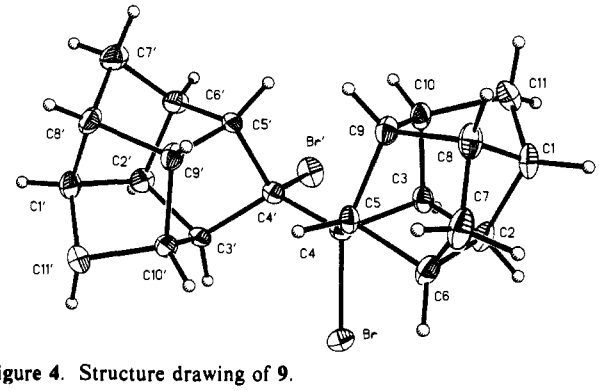

Figure 4. Structure drawing of **9**.

Ostensibly, **10a** resulted from Wagner–Meerwein rearrangement concomitant with bromine addition. If a rearranged *gem*-dibromospiroalkane indeed was formed in this reaction, it did not survive the workup conditions. Most likely, this compound suffered hydrolysis during workup, thereby affording the observed spiroketone **10a**. Despite our efforts, we were unable to isolate any bromine-containing material from the products obtained via reaction of **2a** with Br_2–CCl_4 solution. A control experiment established that hydrolysis occurred prior to column chromatographic isolation and purification of the product (see Experimental Section).

It is clear from the foregoing that alkenes **2a** and **2b** display remarkably different reactivities toward electrophiles. As a first step toward understanding the basis for this observation, the photoelectron spectra (PES) of **2a** and **2b** were obtained.[7] These spectra are virtually superimposable, and both indicate a first vertical ionization energy (due to ionization from the C=C π-

(7) We thank Professor Rolf Gleiter, Department of Chemistry, University of Heidelberg, for having obtained photoelectron spectra of **2a** and **2b**.

Table I. Crystal and Refinement Data

	2a	2b	5	9
formula	$C_{22}H_{24}$	$C_{22}H_{24}$	$C_{22}H_{26}O$	$C_{22}H_{24}Br_2$
crystal dimension (mm)	0.30 × 0.30 × 0.33	0.30 × 0.35 × 0.45	0.50 × 0.25 × 0.25	0.46 × 0.48 × 0.45
space group	$C2/c$	$P\bar{1}$	$C2/c$	$C2/c$
a (Å)	15.678 (2)	6.315 (1)	23.541 (7)	12.825 (2)
b (Å)	10.365 (2)	10.865 (1)	13.794 (3)	6.620 (1)
c (Å)	12.091 (1)	11.369 (1)	9.702 (2)	20.108 (2)
α (deg)	90.00	102.40 (1)	90.00	90.00
β (deg)	131.53 (1)	92.64 (1)	96.01 (2)	98.38 (1)
γ (deg)	90.00	96.68 (1)	90.00	90.00
V (Å^3)	1471.0 (3)	754.7 (2)	3133.0 (1)	1689.0 (3)
Z	4	2	8	4
d_{calcd} (g cm^{-3})	1.302	1.269	1.299	1.763
$F(000)$	624	312	1328	904
μ (cm^{-1})	0.68	0.66	0.72	47.53
transmission factors	0.722–0.837	0.714–0.827	0.908–0.952	0.650–0.951
2θ range (deg)	3–45	3–45	3–55	3–50
lattice parameters	41.20–44.59	31.14–37.87	22.55–28.89	25.86–28.94
check reflections	(152) ($\bar{9}\bar{1}7$)	($\bar{1}52$) ($\bar{2}3\bar{5}$)	($\bar{7}51$) (840)	(290) (153)
h,k,l range	−16,12; 0,11; 0,12	−6,6; −11,11; 0,12	−30,30; −4,17; 0,12	−15,14; 0,7; 0,23
number reflections	963	1971	3582	1488
number $>3\sigma(I)$	852	1747	2673	1173
number parameter	149	296	312	110
R (R_{all})	0.0306 (0.0362)	0.0329 (0.0381)	0.0602 (0.0821)	0.0418 (0.0598)
R_w (R_w)$_{all}$	0.0465 (0.0588)	0.0450 (0.0458)	0.0514 (0.0534)	0.0506 (0.0651)
$(\Delta/\sigma)_{max}$	0.008	0.044	0.020	0.006
S	0.838	1.677	1.717	1.349
residual peaks (e Å^{-3})	−0.12; 0.17	−0.11; 0.14	−0.25; 0.32	−0.59; 0.52
g(weighting scheme)	0.00283	0.00041	0.00018	0.00069

Table II. Structural Features in Several $R_2C{=}CR_2$ Type Molecules with a Planar Double Bond (The Number in Parentheses Denotes the Standard Deviation of Error in the Last Digit Unless Otherwise Noted)

	$r_{C=C}$,[a] Å	<CC(sp^2)C,[a] deg
12	1.336 (4)[b]	110.4 (2)[b]
2a[c]	1.328 (3)	97.0 (1)
	1.332 [MM2]	98.4 [MM2]
	1.320 [AM1]	98.0 [AM1]
2b[c]	1.322 (2)	96.6 (1)
	1.332 [MM2]	98.4 [MM2]
	1.320 [AM1]	98.0 [AM1]
13	1.307 (3)[d]	63.6 (2)[d]

[a] X-ray determination unless otherwise noted. [b] Swen-Walstra, S. C.; Visser, G. T. *J. Chem. Soc., Chem. Commun.* **1971**, 82. [c] This study. [d] Warner, P.; Chang, S. C.; Powell, D. R.; Jacobson, R. A. *Tetrahedron Lett.* **1981**, *22*, 533.

molecular orbital) of 7.9 eV. This value agrees closely with the corresponding value for the first ionization energy of adamantylideneadamantane (**12**) (i.e., 7.84 eV).[8]

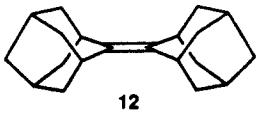

12

Next, cyclic voltammetry (CV) of **2a** and of **2b** was investigated.[9] Both compounds display $E°$ values in CH_2Cl_2–(n-Bu)$_4$N$^+$BF$_4^-$ at room temperature of 1.79 V vs SCE. Peaks that correspond to both oxidation and reduction processes appear in the cyclic voltammograms of **2a** and **2b**.

There is no unusual feature of the PES or the electrochemistry of **2a** and of **2b** that might account for the observed reactivity differences that these compounds display toward electrophiles. Accordingly, we turned to computational methods in an effort to gain theoretical insight into this unusual observation (see Discussion section).

X-ray Structures of 2a, 2b, 5, and 9. The X-ray crystal and refinement data for **2a**, **2b**, **5**, and **9** are given in Table I. Compounds **2a**, **2b**, and **9** each are comprised of two cages (i.e., D_3-trishomocubyl moieties) that are mutually connected by a bond that joins a methylene bridge in one cage with a corresponding methylene bridge in the other. Thus, in **2a** and **2b**, the C(4) and C(4′) methylene bridges in adjacent cage moieties are connected via a C=C double bond, while in **9**, C(4) and C(4′) each bear a bromine atom and are mutually joined via a C–C single bond. Each cage contains three fused norbornane moieties. Experimental and theoretical investigations of norbornanes and of polycyclic molecules that contain one or more norbornane moieties[10] show that the two bonds to the methylene bridge are the shortest C–C bonds while the two C–C bonds that are contained within the ethano bridge are the longest such bonds in the molecule. The four remaining "connecting bonds" (i.e., those C–C bonds that connect the ethano bridges to the bridgehead carbon atoms) are intermediate in length.

In the present study, we find excellent agreement among the various classes of bonds contained within **2a**, **2b**, **5**, and **9**. In **2a**, **2b**, and **9** and in the unrearranged part of **5**, each cage contains six methylene bridge bonds (two of which are adjacent to the bridge positions through which the two cages are joined), three purely connecting bonds, and six bonds which are ethano bonds of one norbornane moiety and connecting bonds of another. The 30 independent ethano-connecting bond types average 1.566 (3) Å, the 15 independent purely connecting bonds average 1.525 (6) Å, and the 20 independent methylene bridge bonds average 1.512 (7) Å. The methylene bridge bonds that are situated adjacent to the connecting double bonds [i.e., C(4) and C(4′) in **2a** and in **2b**] average 1.496 (3) Å. These bonds are internally self-consistent and agree closely with corresponding literature values.

The rearranged half of **5** contains two six-membered rings that exhibit twist and chair conformations, respectively. In addition, **5** contains three five-membered rings in envelope conformations

(8) Mollere, P. D.; Houk, K. N.; Bomse, D. S.; Morton, T. H. *J. Am. Chem. Soc.* **1976**, *98*, 4732.

(9) We thank Professor, Stephen F. Nelsen, Department of Chemistry, University of Wisconsin, for having obtained CV $E°$ values of **2a** and **2b**.

(10) (a) Doms, L.; Van den Enden, L.; Geise, H. J.; Van Alsenoy, C. *J. Am. Chem. Soc.* **1983**, *105*, 158. (b) Doms, L.; Van Hamelrijk, D.; Van de Mieroop, W.; Lenstra, A. T. H.; Geise, H. J. *Acta Crystallogr., Sect. B* **1985**, *41*, 270. (c) Flippen-Anderson, J. L.; Gilardi, R.; George, C.; Marchand, A. P.; Jin, P.-w.; Deshpande, M. N. *Acta Crystallogr., Sect. C: Cryst. Struct. Commun.* **1988**, *44*, 1617. (d) Watson, W. H.; Nagl, A.; Marchand, A. P.; Deshpande, M. N. *Acta Crystallogr., Sect. C: Cryst. Struct. Commun.* **1989**, *45*, 1339. (e) Watson, W. H.; Nagl, A.; Marchand, A. P.; Reddy, G. M.; Reddy, S. P.; Dave, P. R. *Acta Crystallogr., Sect. C: Cryst. Struct. Commun.* **1989**, *45*, 263. (f) Watson, W. H.; Nagl, A.; Marchand, A. P.; Vidyasagar, V. *Acta Crystallogr., Sect. C: Cryst. Struct. Commun.* **1989**, *45*, 1770.

and one additional five-membered ring that exists in a half-chair conformation.

An interesting feature in the X-ray crystal structure of **9** is the fact that two carbon–bromine bonds in this molecule are virtually perpendicular.

In general, observed variations in bond lengths in these cage structures are not well reproduced by the results of MM2 calculations. However, when a torsion–stretch interaction is introduced, this leads to improved agreement between calculated and observed bond length variations in norbornane and related structures.[11]

Discussion

Peculiarities of the C=C Double Bonds in 2a and 2b. The carbon–carbon double bonds in both compounds are essentially planar. Analysis of X-ray crystallographic results revealed that the twist and out-of-plane deformation[12] in **2a** and **2b** are less than 0.2°. However, the C=C bond lengths in these compounds are somewhat shorter than normal. The data in Table II reveal that these bonds are intermediate in length between that of the corresponding C=C bonds in **12** ("normal" length) and in **13** (a cyclopropylidenecyclopropane derivative, which contains the shortest C=C bond among the four compounds in Table II).

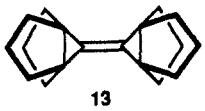

13

The variation among C=C bond lengths parallels the changes in the C(sp^3)–C(sp^2)–C(sp^3) internuclear angles in **2a**, **2b**, **12**, and **13**. Note that C(4) in **2a** and **2b** is contained within a norbornyl moiety; hence, the small valence angle associated with C(4) in these compounds most likely reflects the corresponding C(7) valence angle in norbornane.[13]

A similar trend has been obseerved for a carbon–carbon single bond in dicubyl (**14**)[14] and in a related system.[15] For these R_3C–CR_3 systems, the small RCR valence angle results in a short "intercubyl" C–C bond length. The factors considered to be

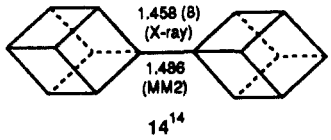

14[14]

responsible for this trend are as follows: (i) Steric repulsion between R groups in **14** is reduced, since these groups are constrained within the cubyl moieties and thereby directed away from the C=C double bond. (ii) The hybridization effect, caused by the high percentage of s character in the carbon orbitals that comprise the intercubyl C–C bond, results in shortening of this bond. The remarkably short intercubyl bond length in **14** [i.e., 1.458 (8) Å] represents an enormous shortening of 0.130 Å vis à vis the average bond length for hexasubstituted ethanes [i.e., 1.588 (25) Å].[16] Structurally MM2-optimized **14** displayed a somewhat greater equilibrium intercubyl bond length [i.e., 1.486 Å].[14] This result indicates that 79% (or 0.102 Å) of the observed C–C bond shrinkage in **14** originates from reduced steric repulsion between R groups [i.e., mechanism (i), above].

In contrast to this result, the corresponding shrinkage of each of the C=C bonds in **2a** and **2b** amounts to only ca. 0.008–0.014 Å when the corresponding C=C bond length in **12** is taken as standard. This result is not surprising, since the C=C bond length

Scheme V

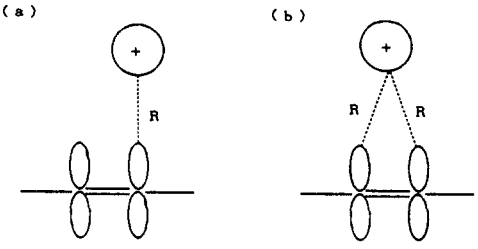

naturally should be less sensitive to steric and hybridization effects than is the corresponding C–C bond length.

The effect of reducing the valence angle produces a dramatic change in the frequency of the C=C stretching vibration.[17] Thus, Raman spectra of **2a** and **2b** revealed the presence of an unusually high absorption band at 1761 cm^{-1}.[18] That this peak is indeed due to the C=C stretching vibration is confirmed by AM1 calculational results, which predict $\nu_{C=C}$ = 1754 cm^{-1} (after an empirical correction factor has been applied; see Computational Techniques in Experimental Section).

Additional evidence that supports our assignment of the band at 1761 cm^{-1} in the Raman spectrum of **2a** and **2b** could be found in the corresponding spectrum of a closely related model compound, 7-norbornylidene-7-norbornane (**15**).[19] Compound **15** was synthesized via titanium-promoted dimerization[2a] of 7-norbornanone.[20] Examination of the Raman spectrum of **15** indicates the C=C stretching vibration to be 1752 cm^{-1}.[18] This value compares closely with the AM1-calculated value of 1755 cm^{-1} for this vibration and is similar to that cited above for the corresponding band in the Raman spectra of **2a** and **2b**.

The remarkably large force constant for the C=C stretching vibration in **2a** and **2b** and in our model compound, **15**, clearly results in each case from the relatively high percentage of s character in the σ-orbital of the C=C double bond. For the same reason, cyclopropylidenecycloalkanes also are known to possess abnormally high C=C stretching frequencies [i.e., 1798 cm^{-1} for **16a**, 1786 cm^{-1} for **16b** and **16c**, and 1776 cm^{-1} for **16d**].[21]

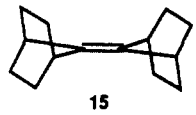

15

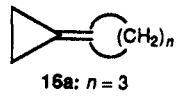

16a: $n = 3$
b: $n = 4$
c: $n = 5$
d: $n = 6$

Electrophilic Attack on 2a and 2b. It is clear from the foregoing that differences between the reactivities of the C=C double bonds in **2a** and **2b** toward electrophiles (Scheme II) cannot be ascribed to vibronic or structural differences. Hence, we look to steric factors in order to explain these reactivity differences.

Several precautionary steps were followed before we attempted to simulate the reaction. However, we were unable to account for the observed reactivity difference in terms of the difference between (i) MM2[5] energies of **2a** and **2b** (see Supplementary Material, Table III) or (ii) MM2 energies of their corresponding protonated species (i.e., **2a**–H^+ and **2b**–H^+, respectively). Similarly, application of appropriate molecular modeling techniques

(11) Allinger, N. L.; Geise, H. J.; Pyckhout, N.; Paquette, L. A.; Gallucci, J. C. *J. Am. Chem. Soc.* **1989**, *111*, 1106.
(12) Ermer, O. *Aspekte von Kraftfeldrechnungen*; Wolfgang Baur Verlag: München, 1981; Chapter 4.
(13) Ōsawa, E.; Barbiric, D. A.; Lee, O. S.; Kitano, Y.; Padma, S.; Mehta, G. *J. Chem. Soc., Perkin Trans. 2* **1989**, 1161.
(14) Gilardi, R.; Maggini, M.; Eaton, P. E. *J. Am. Chem. Soc.* **1988**, *110*, 7232.
(15) Ermer, O.; Lex, J. *Angew. Chem., Int. Ed. Engl.* **1987**, *26*, 447.
(16) Allen, F. H.; Kennard, O.; Watson, D. G.; Brammer, L.; Orpen, A. G.; Taylor, R. *J. Chem. Soc., Perkin Trans. 2* **1987**, S1.
(17) (a) Zefirov, N. S.; Sokolov, V. I. *Russ. Chem. Rev.* **1967**, *36*, 87. (b) The effect of valence angle on the frequency of the C=C stretching vibration is thought to be analogous to the corresponding effect on C=O stretching frequencies in ketones.[17a] However, recent evidence suggests that abnormally high C=O stretching frequencies observed in, e.g., benzaldehyde and acetophenone semicarbazones may be a result of the existence of intermolecular bifurcated hydrogen bonds in the solid state that involve the carbonyl group of these molecules; see: Kolb, V. M.; Stupar, J. W.; Janota, T. E.; Duax, W. L. *J. Org. Chem.* **1989**, *54*, 2341.
(18) We thank Mr. Peng Yuan, Department of Chemistry, University of North Texas, for having obtained the Raman spectra of **2a**, **2b**, and **15**.
(19) Bartlett, P. D.; Ho, M. S. *J. Am. Chem. Soc.* **1974**, *96*, 627.
(20) (a) Gassman, P. G.; Pape, P. G. *J. Org. Chem.* **1964**, *29*, 160. (b) Gassman, P. G.; Marshall, J. L. *Organic Syntheses*; Wiley: New York, 1973; *Collect. Vol. 5*, pp 91, 424.
(21) Vincent, J. P.; Bezaguet, A.; Bertrand, M. *Bull. Soc. Chim. France* **1967**, 3550.

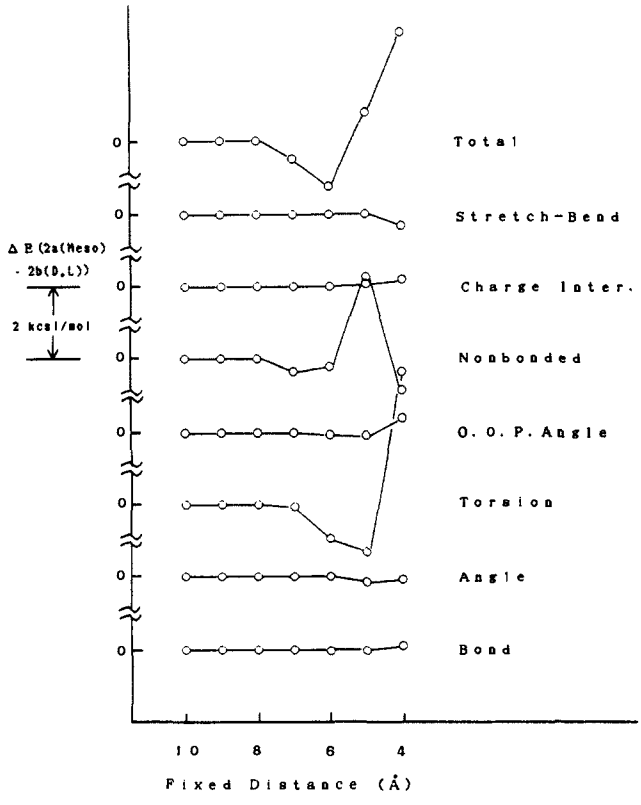

Figure 5. Changes in the relative MM2-derived steric energies, $\Delta E = E(\mathbf{2a}) - E(\mathbf{2b})$ (kcal/mol), with decreasing electrophile–substrate distance, R. Here, R is the distance (in Å) between the solvated proton and an sp^2-hybridized carbon atom in the substrate.

designed to reveal the presence of F strain in **2a** and in **2b** could not account for the observed reactivity difference. Accordingly, an attempt was made by utilizing MM2 to simulate closely the path taken by the electrophile as it approaches the C=C double bond of **2a** and **2b**.

As a first approximation, the solvated electrophile was considered to be a sphere of positive charge that possesses MM2 van der Waals constants of $r_0 = 5$ Å and $\epsilon = 0.5$ kcal/mol. The solvated electrophile was treated as a point charge when calculating electrostatic interactions between the approaching electrophile and the C=C double bond in the substrate. Atomic charges, obtained from AM1 calculations of **2a** and **2b** (see supplementary material, Table IV), were held invariant during the simulation calculations.

Protonation. The solvated proton was placed initially 10 Å above the plane that contains the C=C bond in **2a** and in **2b**, and the composite was geometry-optimized for a given fixed distance, R, between the center of the spherical model of the solvated proton and C(4), i.e., one of the sp^2-hybridized carbon atoms in the substrate (Scheme Va). The distance R then was decreased in 1-Å decrements, and geometry-optimization was repeated at each fixed distance. The distance $R = 4$ Å turned out to be the critical distance beyond which composite geometries could not be optimized due to aggregate strain effects.

Relative energies, $\Delta E = E_{\mathbf{2a}} - E_{\mathbf{2b}}$, are plotted against R in Figure 5. Clearly, the single most important factor responsible for the sharp increase in the energy of **2a** relative to **2b** at R values below 5 Å is the rapid increase in torsional energy of **2a**. The reason for this increase is as follows. Common to **2a** and **2b**, both of the doubly bonded carbon atoms undergo pyrmidalization with approach of the proton (model) as shown in Figure 6 (only for **2a**). Pyramidalization continues at the carbon atom that is undergoing protonation (i.e., the "front" carbon atom) at distances $5 \geq R \geq 4$ Å. This out-of-plane deformation quickly narrows the gap between the two trishomocubyl moieties on either side of the double bond. During this process, **2b** is able to minimize any increase in total strain by introducing a small twist that eventually disappears into the orthogonal conformation of the carbonium ion, **2b**–H^+. However, this option is not available to **2a**, since its two halves are mirror images, and the atoms that face one another across the gap all are mutually eclipsed from the outset. Consequently, the double bond in **2a** is forced to twist toward the planar conformation of the corresponding carbonium ion, **2a**–H^+. In so doing, nonbonded repulsions between γ- and γ'-hydrogen atoms on the back side of the double bond are reduced. Hence, twisting in **2a** proceeds to some extent (at $R = 4$ Å), but this movement is energetically too costly to proceed. Consequently, while **2b** smoothly achieves protonation, **2a** encounters less resistance by undergoing instead antiperiplanar 1,2-shift from one of the pyramidalizing carbon bonds to the incipient cation center in the manner shown in **17**.

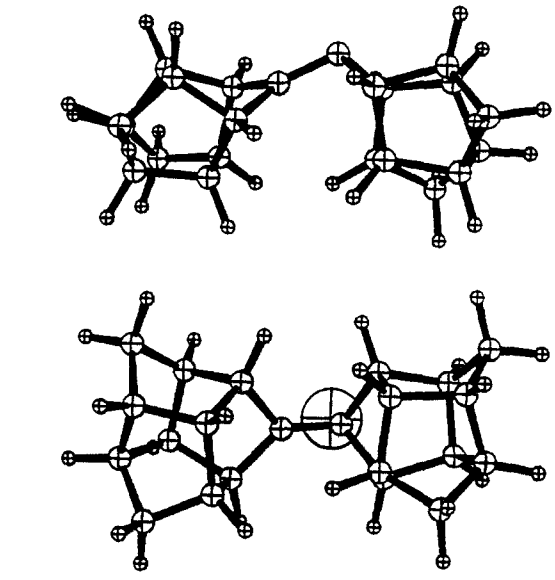

Figure 6. Side and bottom views of MM2-optimized structure of composite (Scheme Va) of solvated proton model and **2a** at $R = 4$ Å. See caption to Figure 5 for the definition of R.

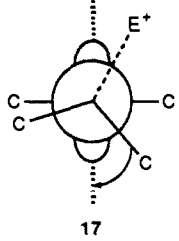

17

Bromination. The bridged brominium ion model[22] shown in Scheme Vb also was studied. The composite constructed in the manner similar to that shown in Scheme Va was geometry optimized while the model electrophile was constrained at a point equidistant from the termini of the C=C double bond. This results in C_s symmetry for the **2a** + Br^+ composite and C_2 symmetry for **2b** + Br^+.

Due to the symmetry conservation rule,[23] the composite **2a** + Br^+ maintained its plane of symmetry throughout geometry optimization at all R values studied. No freedom to twist the double bond exists in this model as had been possible in the corresponding protonation model. Likewise, the initial C_2 axis persists throughout the corresponding **2b** + Br^+ process. In both composites, out-of-plane deformation occurred, and steric energy increased rapidly as R was decreased to 4.5 Å. Geometry optimization failed beyond this critical distance (i.e., for $R < 4.5$ Å). Total energy changed with decreasing R in a manner similar to that which was encountered for the corresponding protonation of **2a** and **2b**. Initially, the **2b** composite is destabilized relative to the corresponding **2a** composite until R reaches 5.5 Å due to torsional strain effects.

(22) Pine, S. H. *Organic Chemistry*, 5th ed.; McGraw-Hill: Tokyo, 1987; p 525.
(23) Ermer, O. *Tetrahedron* **1975**, *31*, 1849.

However, the **2a** composite becomes rapidly destabilized (relative to the **2b** composite) as R is decreased to 4.5 Å due to the cumulative effects of nonbonded repulsion and angle strain.

Beyond this point, nothing can happen unless the initial symmetry constraints are removed. Conceptually, our model must now switch from the "bridged" composite (Scheme Vb) to the "single-footed" structure (Scheme Va), and, at that point, bromination is expected to proceed in a manner that is closely analogous to the mechanism discussed earlier for protonation.[24]

Experimental Section

Melting points are uncorrected.

Titanium-Promoted Dimerization of D_3-Trishomocubanone (1).[2a] To a 100-mL three-neck round-bottom flask was added dry THF (30 mL) under an argon atmosphere. The THF was cooled via application of an external ice bath. To the cooled, stirred solvent was added titanium tetrachloride (2.02 g, 10.5 mmol) via syringe. To the resulting turbid yellow mixture was added powdered zinc (1.43 g, 21.8 mmol) portionwise with stirring. After all of the zinc had been added, the cold bath was removed, and the mixture was heated and refluxed for 1 h. The mixture was then allowed to cool gradually to room temperature, whereupon pyridine (0.5 mL) was added followed by a solution of D_3-trishomocubanone[3] (**1**, 1.6 g, 10 mmol) in dry THF (10 mL). The resulting mixture was refluxed under argon for 24 h. The reaction mixture was then allowed to cool slowly to ambient temperature. The reaction mixture was further cooled via application of an external ice bath, and the cooled solution was quenched via gradual addition of 10% aqueous potassium carbonate solution (ca. 50 mL, excess). The reaction mixture was transferred into a 500-mL conical flask that contained diethyl ether (200 mL). The resulting mixture was stirred vigorously for 10 min and then filtered. The residue was washed thoroughly with ether (2 × 100 mL) and then discarded. The layers in the filtrate were then separated, and the aqueous layer was extracted with ether (2 × 100 mL). The combined ether layers were washed sequentially with water (200 mL), 5% aqueous hydrochloric acid solution (2 × 100 mL), water (2 × 200 mL), and brine (100 mL). The organic layer was dried (anhydrous sodium sulfate) and filtered, and the filtrate was concentrated in vacuo. The residue was purified via careful column chromatography (silica gel stationary phase). Elution with hexane afforded a mixture of *meso*- and *dl*-trishomocubane dimers (**2a** and **2b**, respectively, 864 mg, 60%). Further elution of the chromatography column with chloroform afforded pentacyclo[6.3.0.$0^{2,6}$.$0^{3,10}$.$0^{5,9}$]undecan-4-ol (**3**, 405 mg, 25%), mp 166–168 °C (lit.[4] mp 167–168 °C).

The mixture of dimers **2a** and **2b** was separated by flash column chromatography (silica gel stationary phase, hexane eluent). Under these conditions, the *dl* dimer, **2b**, eluted first from the column, followed shortly thereafter by meso dimer, **2a**. Individual isomers were further purified by fractional recrystallization from hexane. Spectral properties of each isomer are given below:

Dimer 2a (mp 246 °C): IR (KBr) 3006 (s), 2978 (s), 2908 (s), 1465 (w), 1302 (w), 1288 (m), 1276 (w), 1107 (w), 1048 (w), 1034 (w), 980 (w), 794 cm^{-1} (w); ^{1}H NMR (C_6D_6) δ 1.36 (*AB*, J_{AB} = 10.1 Hz, 4 H), 1.42 (*AB*, J_{AB} = 10.1 Hz, 4 H), 1.95–2.08 (m, 8 H), 2.15–2.24 (m, 4 H), 2.35–2.45 (m, 4 H); ^{13}C NMR (C_6D_6) δ 34.24 (t), 42.96 (d), 47.73 (d), 47.75 (d), 49.40 (d), 131.28 (s); mass spectrum (70 eV), *m/e* (relative intensity) 288 (molecular ion, 36.2), 222 (100.0).

Anal. Calcd for $C_{22}H_{24}$: C, 91.61; H, 8.39. Found: C, 91.52; H, 8.41.

Dimer 2b (mp 186 °C): IR (KBr) 2988 (s), 2910 (s), 1466 (w), 1293 (m), 1277 (m), 1050 (w), 978 (w), 795 cm^{-1} (m); ^{1}H NMR (C_6D_6) δ 1.36 (*AB*, J_{AB} = 10.1 Hz, 4 H), 1.42 (*AB*, J_{AB} = 10.1 Hz, 4 H), 1.9–2.5 (m, 16 H); ^{13}C NMR (C_6D_6) δ 34.26 (t), 42.90 (d), 47.71 (d), 47.85 (d), 49.40 (d), 131.22 (s); mass spectrum (70 eV), *m/e* (relative intensity) 288 (molecular ion, 33.9), 222 (100.0).

Anal. Calcd for $C_{22}H_{24}$: C, 91.61; H, 8.39. Found: C, 91.73; H, 8.43.

Addition of Trifluoroacetic Acid to a Mixture of 2a and 2b. To a solution of **2a** and **2b** (ca. 1:1 mixture, 50 mg, 0.17 mmol) in chloroform (15 mL) was added trifluoroacetic acid (TFA, 0.75 mL, 10 mmol, excess), and the resulting mixture was stirred at room temperature for 2.5 h. The reaction was quenched by adding saturated aqueous sodium bicarbonate solution (20 mL) and then was extracted with chloroform (3 × 20 mL). The combined chloroform extracts were washed with water (2 × 30 mL), dried (anhydrous sodium sulfate), and filtered, and the filtrate was concentrated in vacuo. The residue was purified by column chromatography on silica gel (hexane eluent). The first chromatography fraction thereby obtained contained unreacted **2a** (23 mg, mp 246 °C, 46%). Subsequent chromatography fractions afforded adduct **4b** (27 mg, 39%) as a colorless microcrystalline solid: mp 110–111 °C; IR (KBr) 2945 (s), 2862 (s), 1760 (s), 1457 (w), 1365 (m), 1283 (m), 1207 (s), 1160 (s), 857 (w), 773 cm^{-1} (w); ^{1}H NMR ($CDCl_3$) δ 1.32–1.50 (m, 8 H), 1.72–2.00 (m, 17 H); ^{13}C NMR ($CDCl_3$) δ 32.71 (t), 32.97 (t), 33.23 (t), 33.62 (t), 41.62 (d), 41.94 (d), 42.14 (d), 42.99 (d), 45.39 (d), 45.91 (d), 46.63 (d), 46.89 (d), 47.15 (d), 47.34 (d), 47.60 (d), 48.84 (d), 49.55 (d), 50.27 (d), 50.79 (d), 54.17 (d), 55.21 (d), 100.02 (s), 114.77 (q, J_{CF} = 285.2 Hz), 156.21 (q, J_{CF} = 41.3 Hz).

Anal. Calcd for $C_{24}H_{25}F_3O_2$: C, 71.60; H, 6.26. Found: C, 71.74; H, 6.36.

Addition of TFA to 2a. To a solution of isomerically pure **2a** (50 mg, 0.17 mmol) in chloroform (15 mL) was added TFA (0.75 mL, 10 mmol, excess), and the resulting mixture was refluxed for 48 h. The reaction was cooled to room temperature and then was quenched by adding saturated aqueous sodium bicarbonate solution (20 mL). Further workup was performed in the manner described above for the product formed via addition of TFA to a mixture of **2a** and **2b**. The crude product was purified by column chromatography on silica gel (hexane eluent). The first chromatography fraction thereby obtained contained unreacted **2a** (20 mg, mp 246 °C, 40%). Subsequent chromatography fractions afforded **4a** (21 mg, 30%) as a colorless microcrystalline solid: mp 125–126 °C; IR (KBr) 2940 (s), 2865 (s), 1763 (s), 1467 (w), 1363 (w), 1292 (m), 1230 (s), 1178 (s), 1065 (m), 775 cm^{-1} (m); ^{1}H NMR ($CDCl_3$) δ 1.1–2.6 (m, 24 H), 5.12 (d, J = 3.4 Hz, 1 H); ^{13}C NMR ($CDCl_3$) δ 27.47 (t), 33.28 (t), 33.50 (t), 38.44 (t), 39.79 (d), 41.01 (d), 41.43 (d), 41.99 (2 C, d), 42.20 (d), 44.18 (d), 45.16 (d), 45.37 (d), 45.61 (d), 46.88 (d), 47.15 (d), 47.54 (d), 49.87 (d), 50.45 (d), 53.54 (d), 60.63 (s), 78.47 (d), 114.63 (q, J_{CF} = 284.4 Hz), 157.02 (q, J_{CF} = 41.3 Hz).

Anal. Calcd for $C_{24}H_{25}F_3O_2$: C, 71.60; H, 6.26. Found: C, 71.75; H, 6.26.

Lithium Aluminum Hydride Reduction of 4a. A solution of **4a** (80 mg, 0.20 mmol) in dry THF (15 mL) under argon was cooled by application of an external ice–water bath. To this cooled solution was added with stirring lithium aluminum hydride (150 mg, excess). The cold bath then was removed, and the reaction mixture was allowed to warm gradually to room temperature and was stirred at ambient temperature for 16 h. The reaction mixture was cooled (external ice–water bath) and then quenched via successive addition of water (1 mL), 10% aqueous sodium hydroxide solution (1 mL), and water (1.5 mL). The resulting mixture was filtered, and the residue was washed thoroughly with ethyl acetate (ca. 30 mL). The combined filtrates were dried (anhydrous sodium sulfate) and filtered, and the filtrate was concentrated in vacuo. The residue was recrystallized from diethyl ether, thereby affording alcohol **5** (53 mg, 87%) as a colorless microcrystalline solid: mp 184–185 °C; IR (KBr) 3345 (s), 2945 (s), 2877 (s), 1469 (w), 1412 (w), 1299 (m), 1288 (w), 1061 (s), 1038 (m), 977 cm^{-1} (w); ^{1}H NMR ($CDCl_3$) δ 1.07 (dd, J_1 = 11.0 Hz, J_2 = 5.4 Hz, 1 H), 1,16–1.42 (m, 6 H), 1,52 (d, J = 9.5 Hz, 1 H), 1.63–1.81 (m, 4 H), 1.82–2.30 (m, 9 H), 2.31–2.54 (m, 4 H), 3.90 (s, 1 H); ^{13}C NMR ($CDCl_3$) δ 27.68 (t), 33.33 (t), 33.37 (t), 38.47 (t), 40.81 (d), 41.73 (d), 41.79 (d), 41.89 (d), 42.02 (d), 42.82 (d), 44.09 (d), 45.12 (d), 45.37 (d), 46.85 (d), 47.05 (d), 47.47 (d), 48.03 (d), 49.77 (d), 50.44 (d), 53.34 (d), 60.28 (s), 69.55 (d). A crystal of **5**, mp 184–185 °C, obtained via careful recrystallization from diethyl ether, proved to be suitable for X-ray crystallographic analysis (vide infra).

Addition of Bromine to 2b. A solution of bromine (0.5 mL, excess) in carbon tetrachloride (2 mL) was added dropwise with stirring to an ice-cold solution of **2b** (100 mg, 0.347 mmol) in carbon tetrachloride (20 mL). The mixture was warmed to room temperature and stirred for 6 h. The reaction mixture was concentrated in vacuo, and the residue was recrystallized from chloroform. Pure **9** (125 mg, 80%) was thereby obtained as a colorless microcrystalline solid: mp 240° dec; IR (KBr) 3020 (s), 2998 (s), 2977 (s), 2914 (s), 1293 (s), 1280 (m), 1142 (w), 1000 (w), 815 (s), 812 (m), 740 cm^{-1} (s); ^{1}H NMR ($CDCl_3$) δ 1.20–1.56 (m, 8 H), 1.95–2.02 (m, 2 H), 2.13 (m, 4 H), 2.25–2.39 (m, 4 H), 2.53 (m, 2 H), 2.71 (m, 2 H), 3.0 (m, 2 H); ^{13}C NMR ($CDCl_3$) δ 31.69 (t), 32.94 (t), 41.98 (d), 42.79 (d), 44.08 (d), 46.36 (d), 42.83 (d), 50.11 (d), 57.53 (d), 66.44 (d), 87.45 (s).

Anal. Calcd for $C_{22}H_{24}Br_2$: C, 58.95; H, 5.40. Found: C, 59.00; H, 5.30.

Reaction of 2a with Br_2–CCl_4. A solution of bromine (0.5 mL, excess) in carbon tetrachloride (2 mL) was added dropwise with stirring to an ice-cold solution of **2a** (100 mg, 0.347 mmol) in carbon tetrachloride (20 mL). The mixture was warmed to room temperature and stirred for 24 h. The reaction mixture was concentrated by slow evaporation under a stream of argon. The residue that remained was purified by column chromatography (silica gel stationary phase, 5% ethyl acetate–hexane as eluent). Pure spiroketone **10a** (74 mg, 70%) was thereby obtained as a

(24) Changes in the relative MM2-derived steric energies, $\Delta E = E_{2a} - E_{2b}$, with decreasing Br$^+$-substrate distance, R, are shown in Figure 7 (see Supplementary Material).

colorless microcrystalline solid: mp 200–201 °C; IR (KBr) 2983 (s), 2915 (s), 1694 (s), 1473 (w), 1381 (w), 1314 (m), 1299 (m), 1281 (m), 1249 (m), 1216 (w), 1198 (w), 1166 (w), 1100 (w), 828 cm^{-1} (w); ^1H NMR ($CDCl_3$) δ 1.1–1.7 (m, 8 H), 1.8–2.5 (m, 15 H), 3.32 (m, 1 H); ^{13}C NMR ($CDCl_3$) δ 32.83 (t), 33.63 (t), 34.42 (t), 34.66 (t), 35.20 (d), 39.99 (d), 40.60 (d), 41.29 (d), 42.77 (d), 43.80 (d), 45.37 (d), 45.48 (d), 46.06 (d), 46.75 (d), 47.69 (d), 48.28 (d), 49.11 (d), 54.83 (d), 55.94 (d), 57.18 (d), 58.77 (s), 221.14 (s); mass spectrum (70 eV), *m/e* (relative intensity) 304 (molecular ion, 53.9), 238 (100.0).

Anal. Calcd for $C_{11}H_{24}O$: C, 86.80; H, 7.95. Found: C, 86.82; H, 7.85.

Reaction of 2a with Br_2–CCl_4 without Chromatographic Product Workup (Control Study). A control experiment was run to determine whether the observed Wagner–Meerwein rearrangement is concomitant with addition of bromine to the C=C double bond in **2a** or if it occurs instead during column chromatographic workup of the reaction mixture (vide supra). Accordingly, the above reaction was repeated by adding bromine (0.25 mL, excess) to a stirred solution of **2a** (40 mg, 0.14 mmol) in carbon tetrachloride (15 mL). After the reaction had run at room temperature for 24 h, the reaction mixture was concentrated in vacuo. Water (15 mL) was added to the residue, and the resulting mixture was extracted with chloroform (3 × 15 mL). The combined organic layers were washed with water (2 × 15 mL), dried (anhydrous sodium sulfate), and filtered. The filtrate was concentrated in vacuo, and the residue was recrystallized from hexane. Pure **10a** (22 mg, 52%) was thereby obtained as a colorless microcrystalline solid: mp 200–201 °C (mp undepressed upon admixture of this material with authentic **10a** that had been synthesized previously by the method described above).

Reaction of D_3-Trishomocubanone (1) with Sodium–Xylene. Small, freshly cut pieces of sodium metal (1.25 g, 54.3 mg atom) were added to a solution of **1** (1.6 g, 10 mmol) in dry xylene (20 mL), and the resulting mixture was refluxed under nitrogen for 48 h. The reaction mixture was allowed to cool to ambient temperature, and the xylene layer was decanted carefully. Water (50 mL) was added to the xylene layer, and the resulting mixture was extracted with benzene (3 × 50 mL). The combined organic extracts were washed with water (2 × 100 mL), dried (anhydrous sodium sulfate), and filtered. The filtrate was concentrated in vacuo, and the residue was purified by column chromatography (silica gel stationary phase, 15% ethyl acetate–hexane mixed solvent as eluent). The following compounds were thereby obtained: D_3-trishomocubanol (**3**, 324 mg, 20%), *meso*-pinacol **11a** (354 mg, 22%, obtained as a colorless microcrystalline solid: mp 220 °C), *dl*-pinacol **11b** (355 mg, 22%, obtained as a colorless microcrystalline solid: mp 230 °C). Analytically pure **11a** and **11b** were obtained by careful fractional recrystallization from ethyl acetate. Spectral characteristics and microanalytical results for **11a** and **11b** are given below:

Compound 11a: IR (KBr) 3463 (s), 2996 (s), 2910 (s), 1393 (w), 1297 (m), 1189 (w), 1148 (m), 828 (w), 793 cm^{-1} (w); ^1H NMR ($CDCl_3$) δ 1.2–1.5 (m, 8 H), 1.62–1.68 (m, 1 H), 1.95–2.32 (m, 13 H), 2.42–2.52 (m, 2 H), 2.57–2.67 (m, 2 H); ^{13}C NMR ($CDCl_3$) δ 32.44 (t), 34.35 (t), 43.13 (d), 43.55 (d), 43.81 (d), 44.97 (d), 46.09 (d), 47.64 (d), 54.58 (d), 55.20 (d), 90.07 (s); mass spectrum (70 eV), *m/e* (relative intensity) (no molecular ion), 304 (53.1), 238 (100.0).

Anal. Calcd for $C_{22}H_{26}O_2$: C, 81.95; H, 8.12. Found: C, 82.27; H, 8.21.

Compound 11b: IR (KBr) 3448 (s), 2996 (s), 2911 (s), 1296 (m), 1192 (w), 1065 (m), 1053 (m), 1038 (m), 792 cm^{-1} (w); ^1H NMR ($CDCl_3$) δ 1.2–1.48 (m, 8 H), 1.65–1.70 (m, 1 H), 1.85–2.20 (m, 13 H), 2.37–2.48 (m, 2 H), 2.60–2.70 (m, 2 H); ^{13}C NMR ($CDCl_3$) δ 32.73 (t), 34.06 (t), 41.67 (d), 43.89 (d), 43.94 (d), 45.59 (d), 46.59 (d), 47.16 (d), 55.21 (d), 56.69 (d), 89.71 (s); mass spectrum (70 eV), *m/e* (relative intensity) (no molecular ion), 161 (31.5), 160 (100.0), 132 (19.7), 91 (14.6), 79 (25.8), 77 (14.6), 66 (21.9).

Anal. Calcd for $C_{22}H_{26}O_2$: C, 81.95; H, 8.12. Found: C, 82.30; H, 8.21.

Acid-Promoted Pinacol Rearrangement of 11a. Compound **11a** (100 mg, 0.311 mmol) was stirred with concentrated sulfuric acid (2 mL) at 0 °C for 1 h. The reaction was quenched by pouring the reaction mixture into cold water. The resulting mixture was extracted with methylene chloride (3 × 30 mL). The combined methylene chloride extracts were washed with water (2 × 50 mL), dried (anhydrous sodium sulfate), and filtered. The filtrate was concentrated in vacuo, thereby affording spiroketone **10a** (79 mg, 84%) as a colorless microcrystalline solid. Recrystallization of this material from hexane afforded pure **10a**; mp 200–201 °C. The material thereby obtained was identical in all respects with the product obtained from the reaction of **2a** with excess bromine–carbon tetrachloride solution, described previously.

Acid-Promoted Pinacol Rearrangement of 11b. The reaction of **11b** (100 mg, 0.311 mmol) with sulfuric acid (2 mL) at 0 °C was performed in the manner described above for the corresponding reaction of **11a**. Workup of the reaction as described above afforded pure **10b** (78 mg, 83%) as a colorless microcrystalline solid: mp 184–185 °C; IR (KBr) 2990 (s), 2910 (s), 1692 (s), 1472 (w), 1384 (m), 1314 (m), 1298 (m), 1284 (m), 1251 (m), 1217 (m), 1196 (m), 1166 (w), 1100 (w), 968 (w), 833 cm^{-1} (w); ^1H NMR ($CDCl_3$) δ 1.10–1.72 (m, 8 H), 1.86–2.44 (m, 16 H); ^{13}C NMR ($CDCl_3$) δ 32.31 (t), 32.65 (t), 34.46 (t), 34.55 (t), 36.55 (d), 39.07 (d), 39.27 (d), 41.81 (d), 43.40 (d), 43.93 (d), 44.50 (d), 44.57 (d), 46.54 (d), 47.03 (d), 47.68 (d), 47.80 (d), 48.17 (d), 53.90 (d), 54.21 (d), 56.07 (d), 60.09 (s), 221.58 (s); mass spectrum (70 eV), *m/e* (relative intensity) 304 (molecular ion, 86.5), 238 (100.0).

Anal. Calcd for $C_{22}H_{24}O$: C, 86.80; H, 7.95. Found: C, 87.21; H, 8.01.

7-Norbornylidene-7-norbornane (15).[24a] To an externally cooled (0 °C) suspension of titanium tetrachloride (945 mg, 5.00 mmol) in dry tetrahydrofuran (20 mL) under argon was added with stirring zinc dust (653 mg, 10.0 mmol). The resulting mixture was allowed to warm gradually to room temperature, and stirring was continued for 30 min. Pyridine (0.25 mL, 3.1 mmol) was added, followed by addition of a solution of 7-norbornanone[20] (550 mg, 5.00 mmol) in dry tetrahydrofuran (5 mL). The reaction mixture was refluxed for 24 h and then allowed to cool to room temperature. The reaction was quenched via addition of excess 10% aqueous potassium carbonate solution (50 mL). The resulting mixture was extracted with methylene chloride (3 × 50 mL). The combined organic extracts were washed sequentially with 10% aqueous hydrochloric acid (30 mL) and with water (2 × 50 mL). The organic layer was dried (anhydrous sodium sulfate) and filtered, and the filtrate was concentrated in vacuo. The residue was purified by column chromatography on silica gel (hexane eluent), thereby affording **15** (112 mg, 24%). Recrystallization of this material from ligroin afforded pure **15** as a colorless microcrystalline solid: mp 139–140 °C (lit[19] mp 137–138 °C); ^{13}C NMR ($CDCl_3$) δ 29.59 (t), 37.08 (d), 130.97 (s). The infrared and proton NMR spectra of this material agreed with the corresponding spectral values reported previously[19] for **15**.

X-ray Crystallographic Analyses of 2a, 2b, 5, and 9. All X-ray data (Table I) were collected on a Nicolet R3M/μ update of a $P2_1$ diffractometer. Intensity data were collected in the ω-scan mode by using a variable scan rate (4–29.3 deg min^{-1}) and graphite-monochromated Mo Kα radiation. Lattice parameters were obtained from a least-squares refinement of 25 reflections. Lorentz–polarization corrections and an ω-scan based empirical absorption correction were applied. The structures were solved by direct methods and were refined by using a block-cascade least-squares technique. Hydrogen atoms were located in difference maps, and the positions and isothermal temperature parameters were refined for structures **2a**, **2b**, and **5**, while H atoms were allowed to ride on the attached atom for structure **9**. The function minimized was $\sum w(|F_o| - |F_c|)^2$, where the weighting factor is given by $w = [\sigma^2(F_o) + gF_o^2]^{-1}$. All computer programs were supplied by Nicolet Instrument Co. for Desktop 30 Microeclipse and Nova 4/C configuration. Atomic scattering factors and anomalous dispersion corrections were taken from the International Tables for X-ray Crystallography.[25]

Computational Techniques. MM2 calculations[5] were performed by using a packaged program, i.e., BIGSTRN-3.[26] MM2 parameters for carbocations were taken from the work of Müller and Mareda.[27] A locally updated modification of MOPAC (version 3.0) was used to perform AM1 calculations.[28] Normal coordinate vibrational analyses were performed with the option PRECISE, which increased the termination criteria of geometry optimization by 100-fold. The C=C stretching vibration frequencies of simple monoolefins were calculated, and the results were compared with the corresponding experimentally observed values. AM1 afforded calculated frequencies that were ca. 15% higher than the observed values. Least-squares analysis gave the following equation: $\nu_{C=C}^{calc} = 0.546\ \nu + 624.6\ cm^{-1}$, wherein ν denotes the raw calculated frequency. This equation produces theoretical frequencies with a standard deviation of error (vis â vis the corresponding observed frequency, in each case) of 11.7 cm^{-1}. Observed[29] and calculated frequencies (ν, cm^{-1}) for a series of alkenes are as follows: ethylene (1623, 1623), propene (1648, 1644), isobutene (1661, 1653), *cis*-2-butene (1681, 1668), *trans*-2-butene (1676, 1660), 2-methyl-2-butene (1681, 1672), 2,3-dimethyl-2-butene (1672, 1657), methylenecyclohexane (1651, 1654), methylenecyclopentane (1657, 1670), methylenecyclobutane (1678,

(25) *International Tables for X-ray Crystallography*; Kynoch: Birmingham, England (present distributor, Reidel: Dordrecht, Holland), 1974; Vol. 4.

(26) Nachbar, R. B., Jr.; Mislow, K. BIGSTRN-3, *QCPE* **1986**, No. 514.

(27) Müller, P.; Mareda, J. *Tetrahedron Lett.* **1984**, *25*, 1703.

(28) Togasi, M.; Rudzinski, J. M.; Slanina, Z.; Ōsawa, E.; Hirano, T. *QCPE Bull.* **1987**, *7*, 8.

(29) Silverstein, R. M.; Bassler, G. C.; Morrill, T. C. *Spectroscopic Identification of Organic Compounds*, 5th ed.; Wiley: New York, 1981; p 173.

1703), and methylenecyclopropane (1780, 1781).

Interactive molecular modeling was performed on a COMTEC DS 300 3-D graphic terminal by using a MOL-GRAPH program package (both obtained from Daikin Kogyo Co.). ORTEP drawings were made by using Johnson's program.[30]

Acknowledgment. We thank the Air Force Office of Scientific Research (Grant AFOSR-88-0132), the Robert A. Welch Foundation (Grant B-963), and the University of North Texas Faculty Research Committee for financial support. O.S.L. and E.Ō. thank the Ministry of Education, Science, and Culture of Japan for a fellowship and a Grant-in-Aid for Scientific Research, respectively. E.Ō. is grateful to Daikin Kogyo Co. for their having donated a molecular modeling system and to Professor S. Sasaki for his having made a VAX workstation available for this study.

(30) Johnson, C. K. ORTEP-II. Report ORNL-5138; Oak Ridge National Laboratory: Oak Ridge, TN, 1976.

Supplementary Material Available: Figure 7 (changes in relative MM2-derived steric energies, $\Delta E = E_{2a} - E_{2b}$ (kcal/mol), with decreasing Br^+–substrate distance, R), Table III (MM2-derived steric energies of **2a** and **2b**), Table IV (net atomic charges on **2a** and **2b** calculated by AM1), Table V (MM2-derived out-of-plane deformation and twist angle in **2a** and **2b** caused by the approach of the model solvated proton to the C=C double bond); Tables VI-X, XII-XVI, XVIII-XXII, and XXIV-XXVIII (tables of atomic coordinates and isotropic thermal parameters, bond lengths, bond angles, anisotropic thermal parameters, H-atom coordinates and isotropic thermal parameters for **2a**, **2b**, **5**, and **9**) (19 pages); observed and calculated structure factors for **2a**, **2b**, **5**, and **9** (Tables XI, XVII, XXIII, and XXIX, respectively) (49 pages). Ordering information is given on any current masthead page.

Cooxidation Reactions during Oxidations of Superoxide with Polyhalides, CO_2, Phosphates, and Acyl Halides

Tetsuo Nagano, Hiroshi Yamamoto, and Masaaki Hirobe*

Contribution from the Faculty of Pharmaceutical Sciences, University of Tokyo, Hongo, Bunkyo-ku, Tokyo 113, Japan. *Received June 5, 1989. Revised Manuscript Received December 19, 1989*

Abstract: Superoxide ($O_2^{\bullet-}$) reacted with polyhalides, CO_2, phosphates, and acyl halides to form the corresponding peroxy intermediates, which could be used as reactive oxidants. Polyhalides reacted with $O_2^{\bullet-}$ to cause cooxidation of olefins to the corresponding oxides in good yields. The yields of the oxides correlated well with the reactivities of polyhalides with $O_2^{\bullet-}$. The reactions of CO_2 and phosphates with $O_2^{\bullet-}$ caused cooxidation of sulfides to the sulfoxides and that of sulfoxides to the sulfones, respectively, in high yields. The mechanisms of these reactions were examined with the use of $K^{18}O_2$. Acyl halides were found to have nucleophilic attack of $O_2^{\bullet-}$ to generate acylperoxy radicals and anions. On the other hand, CCl_4 as a polyhalide, CO_2, and phosphates in the reaction with $O_2^{\bullet-}$ seemed to form $CCl_3^{\bullet}$, $CO_2^{\bullet-}$, and phosphate anion radicals, respectively, which were followed by addition of O_2 to form the corresponding hydroperoxides or peroxy anions as potent oxidants. These results seem to indicate that $O_2^{\bullet-}$ acts as a nucleophile and a one-electron reductant. Also, the relative rate constants were measured by the rotating ring–disk voltammetric method. The orders of magnitude for pseudo-first-order rate constants $k_1/[s]$, were 10^4, 10^3, and 10^1 in the reactions of $O_2^{\bullet-}$ with acyl halides, CCl_4, and phosphates, respectively. There was a good correlation between $k_1/[s]$ and product yields in the cooxidation of *trans*-stilbene by systems of $O_2^{\bullet-}$ and acyl halides or anhydrides.

Superoxide ($O_2^{\bullet-}$), an active oxygen species, is generated universally in biological systems. It plays important roles in various diseases caused by oxygen toxicity such as ischemia,[1] carcinogenesis,[2] inflammation,[3] diabetes,[4] and aging.[5] During the past two decades, considerable interest has been focused on the chemistry and the reactivity of $O_2^{\bullet-}$ by many chemists and biochemists. $O_2^{\bullet-}$ has diverse reactivities;[6] in aqueous media, it is a Brønsted base[7] and dismutates to H_2O_2 and O_2,[8] while in aprotic media, $O_2^{\bullet-}$ acts as an effective nucleophile[6,9] or causes labile hydrogen abstraction in addition to dismutation.[10] Moreover, $O_2^{\bullet-}$ can act as a one-electron reductant[9,11] or a one-electron oxidant.[12] There are many reports of $O_2^{\bullet-}$ being very toxic to living cells,[13] but the reactivity of $O_2^{\bullet-}$ alone is not as vigorous in vitro as those of other active oxygen species, e.g., $^{\bullet}OH$, $^1O_2$.[6]

We have reported that the acylperoxy radical [$RC(O)OO^{\bullet}$] or acylperoxy anion [$RC(O)OO^-$], generated in situ by treatment of acyl halide with $O_2^{\bullet-}$, is much more reactive than $O_2^{\bullet-}$ alone.[14] Sawyer et al. have reported that, in aprotic solvents, $O_2^{\bullet-}$ can oxygenate CCl_4 or CO_2 to yield peroxy intermediates ($CCl_3OO^{\bullet}$ and CCl_3OO^-, $CO_4^{\bullet-}$ and $C_2O_6^{\bullet-}$).[10,15,16] We have found that $O_2^{\bullet-}$ oxidizes various substrates in the presence of polyhalides or CO_2[17] and also causes serious damage to biological systems in the presence of CCl_4.[18] Thus, the peroxy intermediates were revealed to be more reactive than $O_2^{\bullet-}$ alone. Furthermore, we have reported that the phosphate moiety of nucleotides enhances the reactivity of $O_2^{\bullet-}$ in the nucleobase release reaction of nucleotides.[19]

* To whom correspondence should be addressed.

(1) (a) Nishida, T.; Sibata, H.; Koseki, M.; Kawashima, Y.; Yoshida, Y.; Tagawa, K. *Biochim. Biophys. Acta* **1987**, *890*, 82–88. (b) Hess, M. L.; Okabe, E.; Philip, A.; Kontos, H. A. *Cardiovasc. Res.* **1984**, *18*, 149–157. (c) Hess, M. L.; Okabe, E.; Kontos, H. A. *J. Mol. Cell Cardiol.* **1981**, *13*, 767–772. (d) Feher, J. J.; Briggs, F. N.; Hess, M. L. *J. Mol. Cell Cardiol.* **1980**, *12*, 427–432. (e) Aishia, H.; Morimura, T.; Obata, T.; Miura, Y.; Miyamoto, T.; Tsuboshima, M.; Mizushima, Y. *Arch. Int. Pharmacodyn. Ther.* **1983**, *261*, 316–326.

(2) (a) Cerutti, P. A. *Science* **1985**, *227*, 375–381. (b) Miller, R. C.; Osmak, R.; Zimmerman, M.; Hall, E. J. *Int. J. Rad. Oncol., Biol., Phys.* **1982**, *8*, 771–775. (c) Schwarz, M.; Peres, G.; Kunz, W.; Furstenberger, G.; Kittstein, W.; Marks, F. *Carcinogenesis* **1984**, *5*, 1663–1670. (d) Weitzman, S. A.; Weitberg, A. B.; Clark, E. P.; Stossel, T. P. *Science* **1985**, *227*, 1231–1233.

(3) (a) McCord, J. M. *Agent Actions* **1980**, *10*, 522–527. (b) McCord, J. M.; Wong, K.; Stokes, S. H.; Petrone, W. F.; English, D. In *Pathology of Oxygen*; Autor, A. P., Ed.; Academic Press: New York, 1982; pp 75–81. (c) McCord, J. M.; Stokes, S. H.; Wong, K. *Adv. Inflammation Res.* **1979**, *1*, 273–278.

(4) (a) Fischer, L. J.; Hamburger, S. A. *Diabetes* **1980**, *29*, 213–216. (b) Robbins, M. J.; Sharp, R. A.; Slonim, A. E.; Burr, I. M. *Diabetologia* **1980**, *18*, 55–58. (c) Slonim, A. E.; Surbur, M. L.; Page, D. L.; Sharp, R. A.; Burr, I. M. *J. Clin. Invest.* **1983**, *71*, 1282–1288. (d) Asayama, K.; English, D.; Slonim, A. E.; Burr, J. M. *Diabetes* **1984**, *33*, 160–163. (e) Malaisse, W. J.; Malaise-Lagae, F.; Sener, A.; Pipeless, D. G. *Proc. Natl. Acad. Sci. U.S.A.* **1982**, *79*, 927–930.

(5) (a) Bartosz, G.; Leyko, W.; Fried, R. *Experientia* **1979**, *35*, 1193. (b) Kellog, E. W., III; Fridovich, I. *J. Geronotol.* **1976**, *31*, 405–408.

0002-7863/90/1512-3529$02.50/0